Original Article

arm
Annals of Rehabilitation Medicine

Resting-State Metabolism of Hand Knob Area on ^{18}F-FDG PET-CT According to Hand Function and Tractography of Corticospinal Tract After Stroke

Hae Won Kim, MD[1], Dong Gyu Lee, MD[2]

[1]Department of Nuclear Medicine, Keimyung University School of Medicine, Daegu;
[2]Department of Physical Medicine and Rehabilitation, Yeungnam University College of Medicine, Daegu, Korea

Objective To correlate the resting metabolism of hand knob and hand function after stroke, diffuse tensor tractography (DTT) and ^{18}F-fluorodeoxyglucose position emission tomography (^{18}F-FDG PET) were used to evaluate constructible state of white matter tract and metabolic state of gray matter, respectively.

Methods A total of 17 patients were included in the study, who had suffered a stroke with hand weakness, after a stroke. They underwent diffusion tensor analysis and FDG PET in the subacute period. The ratio of both hemisphere parameters in voxel number of fibers, fractional anisotropy (FA) and apparent diffusion coefficient obtained by corticospinal tract as constructed by DTT, and the metabolism of hand knob area on cerebral cortex obtained from ^{18}F-FDG PET were calculated. Hand movement scale was evaluated on the day of FDG PET or tractography, and at 6 months after onset.

Results Difference of FA in DTT between both hemispheres and hand knob metabolism in FDG PET significantly correlated with the hand movement scale at the subacute stage and 6 months after onset. However, the difference of both hemispheres in DTT and metabolism of hand knob area was not significant.

Conclusion Resting metabolism on hand knob in FDG PET correlated with hand function after stroke.

Keywords Stroke, Diffusion tractography, Fluorodeoxyglucose, Positron emission tomography

INTRODUCTION

Predicting motor recovery after stroke is important for determining the strategy of rehabilitation and the effec-

tiveness of the therapeutic tools provided to the survivor [1]. The lateral corticospinal tract (CST) is an essential pathway for the motor activity of the extremities, and the quantitative and qualitative evaluation of CST is helpful

to assess the state of injury and motor outcome after a stroke. Diffusion tensor tractography (DTT) calculates the quantitative parameters and visualizes anatomical integrity of white matter tract. It evaluates changes of CST after stroke [2], and is helpful in predicting motor outcome after a stroke [3]. However, DTT has a limitation in clinical application as it requires multistep processing, which can distort real information [4]. Moreover, evaluation of CST is difficult if a brain injury is located close to a cortical lesion. Hence, efforts are underway to find additional tools that are effective and objective in estimating the extent of injury after a stroke.

Neuroplasticity gives rise to a variety of dynamic changes at the cerebral cortex, as the brain tries to recover from neural injury. After a stroke, functional magnetic resonance imaging (MRI) provides a read of active and dynamic metabolic changes in the cerebral cortex, associated when a subject attempts at motor performance of an extremity. For a more direct measure, ^{18}F-fluorodeoxyglucose (^{18}F-FDG) position emission tomography (PET) shows the resting-state cerebral metabolic rate for glucose metabolism, and helps in pinpointing the hypometabolism at a cortical lesion site after a stroke [5]. Studies have demonstrated a correlation between cortical metabolic changes and a functional motor deficit. Hence, we proposed to use the ^{18}F-FDG PET to study cortical metabolic changes at hand knob area according to hand function, and investigate the validity of ^{18}F-FDG PET in predicting hand motor outcome after stroke, as compared with the more commonly used DTT to predict motor outcome.

MATERIALS AND METHODS

Subjects

Seventeen patients (9 females and 8 males; mean age, 60.18±13.54 years; 5 with ischemic strokes and 12 with hemorrhagic strokes) were enrolled in this study (Table 1). All patients provided their written informed consent prior to the study. The study protocol was approved by the local ethics committee. Stroke had previously been identified by a CT scan or an MRI. Additional eligibility for patients who had motor weakness in the hemiside, required agreement to undergo ^{18}F-FDG PET and diffusion tensor imaging. The following exclusion criteria were applied: preexisting neurologic and psychologic deficits, an existing neurologic condition, or a medical state precluding ^{18}F-FDG PET and diffusion tensor scans.

Scale for hand movement

A hand movement scale (HMS) was used to evaluate hand function at the subacute phase (25.3±12.1 days) and 6 months after onset of stroke. HMS is graded and classified on a scale 1 to 6, as follows: 1, no active movement in digits; 2, active flexion of all fingers in synergy only; 3, active flexion and extension of all fingers in synergy; 4, ability to extend the index finger while maintaining the other fingers in flexion; 5, ability to bring the thumb into opposition to the tip to the index finger only; and 6, ability to oppose thumb to all fingertips [6].

Diffusion tensor tractography

Diffusion tensor image was acquired using a sensitivity-encoding head coil on a 3.0T MR scanner (GE Healthcare, Waukesha, WI, USA). A diffusion-weighted echo-planar imaging sequence was performed with the following parameters, for each of the 26 noncollinear diffusion-sensitizing gradients: TR/TE/NEX, 10000 ms/95.9 ms/2.0; slice thickness, 2.6 mm; b=1000 s/mm^2; matrix 128×128; FOV, 250 mm×250 mm. Eddy current-induced image distortions were removed using affine multi-scale two-dimensional registration in the Oxford Centre for Functional Magnetic Resonance Imaging of the Brain (FMRIB) Software Library (FSL; www.fmrib.ox.ac.uk/fsl). Fiber tracking was performed using DTI-Studio software (CMRM at John Hopkins Medical Institute, Baltimore, MD, USA) for reconstruction of the CST by a fraction anisotropy <0.2, and angle change >60°. Seed region of interest (ROI) was drawn in the anatomical CST portion in the anterior mid pons on the color map, and another ROI was drawn in the anatomical CST portion in the lower pons. Numbers for fiber voxel, fractional anisotropy (FA), and apparent diffusion coefficient (ADC) were calculated from CST constructed by DTT. The difference for each parameter between hemispheres was calculated as the difference between ipsilateral and contralateral hemisphere.

^{18}F-FDG PET images

The ^{18}F-FDG PET scan was performed with a Biograph mCT-64 PET/CT camera (Siemens Healthcare, Knoxville, TN, USA) in a quiet and dimly lit room. All subjects fasted for at least 6 hours before the scan. Image acquisition was

Table 1. Demographic, clinical, ^{18}F-FDG PET and DTT parameters of subjects

Patient no.	Sex/age	Lesion side	Stroke etiology	Days from stroke to PET	MR_{gluc} [a] of ^{18}F-FDG PET	DTT difference of between hemispheres			Hand movement scale	
						Voxel[b]	FA	ADC	PET check day	At 6 months
1	F/54	Rt	Hemorrhage	33	0.15	206	0.02	0.08	5	6
2	M/68	Lt	Hemorrhage	24	0.08	37	0.04	0.05	5	6
3	M/74	Rt	Hemorrhage	23	0.16	144	0.03	0.04	5	6
4	M/61	Rt	Hemorrhage	41	0.12	1,002	0.02	0.05	5	6
5	F/64	Rt	Hemorrhage	18	0.15	1,821	0.07	0.09	4	6
6	M39	Rt	Hemorrhage	15	0.17	813	0.12	0.19	5	6
7	F/54	Rt	Hemorrhage	14	0.19	391	0.01	0.01	5	6
8	M/76	Rt	Hemorrhage	18	0.09	388	0.03	0.02	5	6
9	F/54	Rt	Ischemia	21	0.11	566	0.04	0.08	5	6
10	F/76	Rt	Ischemia	24	0.19	256	0.03	0.06	5	6
11	F/60	Lt	Hemorrhage	14	0.23	124	0.04	0.03	2	5
12	F/32	Rt	Hemorrhage	24	0.32	1,117	0.03	0.06	1	3
13	M/80	Lt	Ischemia	30	0.31	1,898	0.02	0.02	2	3
14	M/64	Lt	Hemorrhage	38	0.35	1,715	0.53	0.70	1	1
15	F/60	Rt	Ischemia	60	1.12	203	0.12	0.12	1	1
16	F/66	Rt	Ischemia	18	0.67	693	0.15	0.15	1	1
17	M/41	Rt	Hemorrhage	15	0.23	2,230	0.26	0.43	1	2

DTT, diffusion tensor tractography; ^{18}F-FDG PET, ^{18}F-fluorodeoxyglucose position emission tomography; FA, fractional anisotropy; ADC, apparent diffusion coefficient; VOI, volume of interest.

[a] MR_{gluc} was defined as follow: MR_{gluc}=(contralateral hemisphere count of regional VOI/count of whole brain on ^{18}F-FDG PET)–(ipsilateral hemisphere count of regional VOI/count of whole brain on ^{18}F-FDG PET).

[b] Voxel is the number of fiber voxel in corticospinal tract constructed by DTT.

started 30 minutes after intravenous injection of ^{18}F-FDG (185 MBq). Brain CT was performed in the spiral mode at 120 kVp and 150 mAs. Subsequently, emission PET data were acquired for 5 minutes in the three-dimensional mode. The transaxial field of view was 25 cm, and the matrix size was 128×128. The spatial resolution in the air was 2.14 mm full width half maximum. ^{18}F-FDG PET images were reconstructed iteratively by the ordered subset expectation maximization method.

For quantitative analyses of the ^{18}F-FDG PET scan, image processing was performed with the SPM2 (Wellcome Trust Centre for Neuroimaging at University College London, UK) within MATLAB 2013a (MathWorks, Natick, MA, USA). Quantitative analyses were based on volumes-of-interest (VOIs). All reconstructed PET images were spatially normalized to the Montreal Neurology Institute (MNI) template space by use of a standard ^{18}F-FDG PET template.

Using a canonical spatially-normalized T1 MRI (GE Healthcare), two VOIs of the bilateral precentral 'hand knob' areas were defined by us. The volume of a precentral 'hand knob' area was 0.7 cm^3. To ensure the registration accuracy, the positions of automatically defined template VOIs were manually adjusted by VOI editing software, PMOD (PMOD Technologies Ltd, Zurich, Switzerland) [5]. The activity concentration in each VOI of the ^{18}F-FDG PET images was calculated, with whole brain as a reference count, via the automated anatomic labeling template. The difference of regional glucose metabolic difference (MR_{gluc}) was defined as follow: MR_{gluc}=(contralateral hemisphere count of regional VOI/count of whole brain on ^{18}F-FDG PET)–(ipsilateral hemisphere count of regional VOI/count of whole brain on ^{18}F-FDG PET). The count was defined as counts per voxel in each VOI, specifically in unit of Bq/mL.

Statistical analysis

The Spearman correlation test was used to determine the relationship between DTT parameters ratio and HMS, indicating the metabolism of hand knob area on ^{18}F-FDG PET and HMS, respectively, using the SPSS ver. 23 for Window (IBM, Armonk, NY, USA). A p-value of less than 0.05 was regarded as statistically significant. MR_{gluc} of ^{18}F-FDG PET and parameters ratio of DTT was used for statistical analysis. To determine the correlation between DTT and metabolism of ^{18}F-FDG PET, the Pearson correlation test was also used. According to continuity of CST constructed by DTT, the results were classified into two groups: complete interrupted and uninterrupted group. Uninterrupted CST indicated that the CST originated from the cerebral cortex to medullar region, even though any part of CST tractography is interrupted. Mann-Whitney U-test was used to validate MR_{gluc} according to the groups, to predict motor outcome.

RESULTS

Tractography and hand function

Statistically significant correlation was observed between FA ratio of bilateral CST and HMS, at PET check day and 6 months after onset (Table 2). However, other variants in CST tractography did not show any significant correlation compared to HMS, except ADC which showed significant correlation at 6 months after onset.

MR$_{gluc}$ in hand knob area and hand function

MR_{gluc} in hand knob area on ^{18}F-FDG PET showed a statistically significant correlation with HMS at the subacute stage (p<0.008) and at 6 months after onset (p=0.000) (Table 2). MR_{gluc} in hand knob area on ^{18}F-FDG PET showed high correlation coefficient values at PET check day and 6 months after onset (Fig. 1). However, there was no significant correlation between MR_{gluc} and ages.

MR$_{gluc}$ in hand knob area and tractography

To identify the relationship between structural change of CST and metabolic change of cortical hand knob area, we evaluated the correlation between variants of CST tractography and MR_{gluc} of ^{18}F-FDG PET. Comparison and correlation between variants of CST tractography and MR_{gluc} of ^{18}F-FDG PET were not statistically significant (Table 3). Interrupted CST in DTT after stroke was seen in 5 patients. Interrupted groups and uninterrupted groups had 0.54±0.37 and 0.16±0.07 of mean difference of MR_{gluc}, respectively. Hence, a statistically significant difference of MR_{gluc} between interrupted and uninterrupted CST group in DTT (p<0.05) was observed. Difference of MR_{gluc} had no correlation with the quantitative variants of CST tractography, but significant correlation was seen with regards to interrupted or uninterrupted CST tractography. Interrupted CST profoundly produced suppression of resting state metabolism on the hand knob area.

Table 2. The correlation coefficient of HMS at PET-CT day and 6 months after onset, and variants of DTT and ^{18}F-FDG PET

Variant	PET day		6 months after onset	
	r_s	p-value	r_s	p-value
DTT				
Difference of number of voxels[a] between both hemispheres[b]	-0.431	0.084	-0.322	0.207
Difference of FA between both hemispheres[b]	-0.579	0.015*	-0.557	0.020*
Difference of ADC between both hemispheres[b]	-0.473	0.055	-0.446	0.073
PET				
Difference of metabolism in both hand knob areas[c]	0.879	0.008*	0.836	0.000*

HMS, hand movement scale; DTT, diffusion tensor tractography; ^{18}F-FDG PET, ^{18}F-fluorodeoxyglucose position emission tomography; CT, computed tomography; FA, fractional anisotropy; ADC, apparent diffusion coefficient; VOI, volume of interest.
[a]Voxels are the numbers of fiber voxel in corticospinal tract constructed by DTT.
[b]Absolute value of difference between hemispheres.
[c]Difference of metabolism between hand nob areas=(contralateral hemisphere count of regional VOI/count of whole brain on ^{18}F-FDGPET)–(ipsilateral hemisphere count of regional VOI/count of whole brain on ^{18}F-FDGPET).
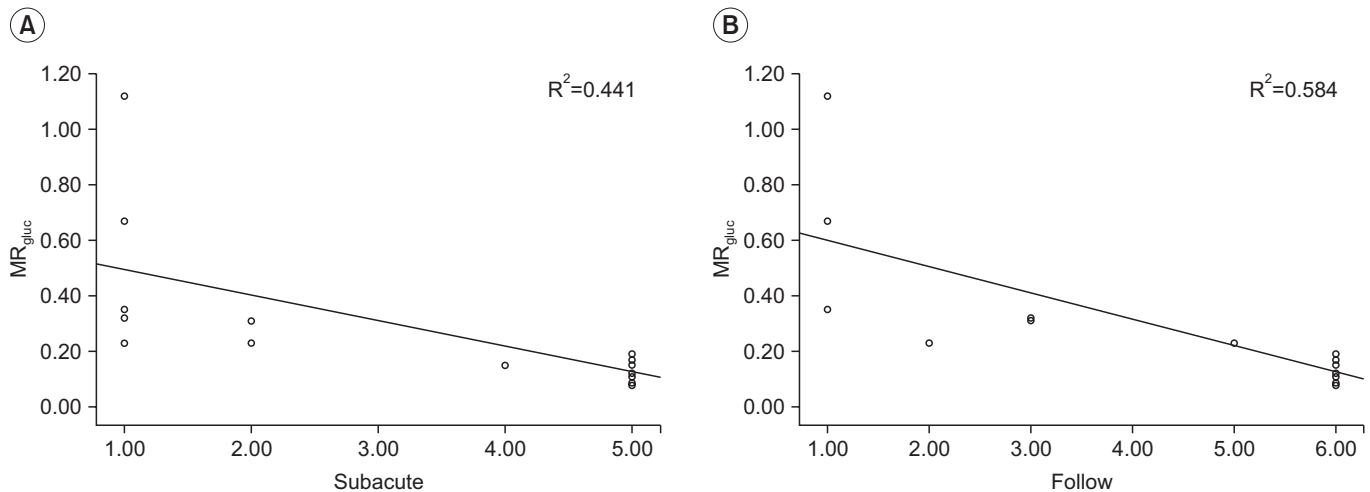*p<0.05.

Fig. 1. The correlation between hand knob regional glucose metabolic and hand movement scale at the subacute phase (A) and 6 months after onset (B). ^{18}F-FDG PET, ^{18}F-fluorodeoxyglucose position emission tomography; VOI, volume of interest. MR_{gluc}=(contralateral hemisphere count of regional VOI/count of whole brain on ^{18}F-FDG PET)–(ipsilateral hemisphere count of regional VOI/count of whole brain on ^{18}F-FDG PET).

Table 3. Comparison between variants of tractography and hand knob metabolism of ^{18}F-FDG PET

Variant	r_s	p-value
Correlation of metabolism and voxels[a] between both hemispheres	-0.442	0.872
Correlation of metabolism and FA between both hemispheres	0.256	0.321
Correlation of metabolism and ADC between both hemisphere	0.155	0.553

^{18}F-FDG PET, ^{18}F-fluorodeoxyglucose position emission tomography; FA, fractional anisotropy; ADC, apparent diffusion coefficient.
[a]Voxels are the numbers of fiber voxels in corticospinal tract constructed by diffusion tensor tractography.

DISCUSSION

The brain is a network of distributed neural components, whose interaction produces and controls motor behavior [7]. After brain injury, these functional and anatomical connectivity elicit cortical metabolic and structural changes within the ipsilateral hemisphere, and between ipsilateral and contralateral hemispheres. Functional MRI (fMRI), transmagnetic stimulation, diffusion tensor tractography, and PET have been widely performed to investigate the cortical activation changes relative to injury, and the recovery mechanism of motor function after stroke [8].

In fMRI, laterality index (LI) is used to estimate the dominance of performance for a pair of connected areas [9]. Based on this notion, we estimated the MR_{gluc} of hand knob area in primary motor cortex to assess the resting state of metabolism on ^{18}F-FDG PET. Precentral knob is well known as a reliable anatomical area that represents

the primary motor cortex of the hand in precentral gyrus [10]. Identification of hand knob area in the axial plane has 98%–100% sensitivity and accuracy. Therefore, we calculated the resting state metabolism of hand knob at fused axial PET scan with MRI

In order to investigate changes in motor cortical activity by fMRI, it is required that the subject be able to make a typical movement, relevant to the target area in the motor cortex. However, ^{18}F-FDG PET can detect information of resting state metabolism even derived from patients unable to perform a given task, such as after a stroke. Hence, we estimated the cortical resting hand knob metabolism on ^{18}F-FDG PET to predict motor outcome post-stroke at the subacute stage, even for subjects who were unable to perform hand movements.

In a study such as ours, reference tissue assignment is important for quantitative assessment of the glucose metabolism, since variability of the activity concentration in the reference tissue greatly affects the study results,

leading to erroneous conclusions [11]. In the current study, the whole brain was used as a reference region for quantitative analysis of ^{18}F-FDG PET, and the MR_{gluc} could be calculated in a consistent manner. Although patients with stroke had multiple regions of decreased glucose metabolism in the cortical and subcortical areas of the bilateral cerebral hemisphere as well as in the brain stem and both cerebellum regions, the normalization to the whole brain minimizes the variability of the activity concentration in the precentral 'hand knob' areas. Several studies with quantitative analysis using proportional scaling to the global mean have presented the diagnostic value of ^{18}F-FDG PET in patients with varying kinds of brain disorders, such as Alzheimer disease, Parkinson disease, epilepsy and stroke [12].

DTT can visualize the continuity of CST and three-dimensional relationships between infarct territory and CST. Several studies indicate that DTT can be used to predict motor performance outcome after stroke [13]. Moreover, integrity of CST is an important factor to predict motor outcome. Cho et al. [3] reported that subjects who have interrupted CST in DTT presented poor clinical outcome compared to intact continuity CST. Based on these factors, we estimated an association between parameters of CST in DTT and MR_{gluc} in PET. However, there were no statistically significant correlations between the quantitative parameters of CST and MR_{gluc}. Only metabolic differences between interrupted and uninterrupted groups had statistical significance, indicating that interrupted CST profoundly influences the resting cortical metabolism. Quantitative parameters of CST were unrelated to MR_{gluc}, but a statistically significant correlation was seen between FA ratio of bilateral CST and HMS at PET check day and 6 months after onset. These results explain that the resting metabolism of hand knob area is not quantitatively associated with CST tractography, but is associated with severe CST injury such as interrupted tractography. Hence, we propose that the resting metabolism of hand knob area is influenced not only by CST, but also functionally and anatomically connected lesions. However, the scanning day of diffusion tensor after stroke also varies from the PET check day; hence, the quantitative results of each parameters will change according to recovery of motor function and/or injury mechanism.

This study provides supporting evidence that ^{18}F-FDG PET can predict motor outcome after stroke while

comparing CST constructed by DTT. We also show that changes of hand knob metabolism on PET can be used to predict hand motor outcome at the subacute stage post-stroke. Our study, however, has several limitations. First, our study had a relatively small pool of patients. As such, the statistical power of subgroup analysis for interrupted and uninterrupted subjects was weak. Second, our subjects were heterogeneous, with respect to either having had ischemic or hemorrhagic stroke. Hence, there is a possibility of each stroke type having differences in cortical metabolism, which were not addressed in this study. Third, we did not evaluate ^{18}F-FDG PET at a specific time point after stroke, resulting in the PET check day after stroke being varied from 14 to 60 days, which could possibly influence changes of resting state metabolism at hand knob area. To validate the prognostic usefulness of ^{18}F-FDG PET with hand function after stroke, PET scanning at a fixed time after stroke is required. Even with these limitations, this study is the first to report a correlation between hand knob metabolism in ^{18}F-FDG PET and state of CST after stroke, and the results provide a better understanding of resting state cortical metabolic changes after stroke, and improved prognosis for motor function recovery for the patient.

CONFLICT OF INTEREST

No potential conflict of interest relevant to this article was reported.

REFERENCES

1. Langhorne P, Coupar F, Pollock A. Motor recovery after stroke: a systematic review. Lancet Neurol 2009;8: 741-54.

2. Mori S, Crain BJ, Chacko VP, van Zijl PC. Three-dimensional tracking of axonal projections in the brain by magnetic resonance imaging. Ann Neurol 1999;45:265-9.

3. Cho SH, Kim DG, Kim DS, Kim YH, Lee CH, Jang SH. Motor outcome according to the integrity of the corticospinal tract determined by diffusion tensor tractography in the early stage of corona radiata infarct. Neurosci Lett 2007;426:123-7.

4. Herrero MT, Barcia C, Navarro JM. Functional anatomy of thalamus and basal ganglia. Childs Nerv Syst

2002;18:386-404.

5. Dimitrakopoulou-Strauss A, Strauss LG, Burger C. Quantitative PET studies in pretreated melanoma patients: a comparison of 6-[18F]fluoro-L-dopa with 18F-FDG and (15)O-water using compartment and noncompartment analysis. J Nucl Med 2001;42:248-56.

6. Katrak P, Bowring G, Conroy P, Chilvers M, Poulos R, McNeil D. Predicting upper limb recovery after stroke: the place of early shoulder and hand movement. Arch Phys Med Rehabil 1998;79:758-61.

7. Felleman DJ, Van Essen DC. Distributed hierarchical processing in the primate cerebral cortex. Cereb Cortex 1991;1:1-47.

8. Jang SH, Cho SH, Kim YH, Kwon YH, Byun WM, Lee SJ, et al. Cortical activation changes associated with motor recovery in patients with precentral knob infarct. Neuroreport 2004;15:395-9.

9. Seghier ML. Laterality index in functional MRI: methodological issues. Magn Reson Imaging 2008;26:594-

601.

10. Yousry TA, Schmid UD, Alkadhi H, Schmidt D, Peraud A, Buettner A, et al. Localization of the motor hand area to a knob on the precentral gyrus: a new landmark. Brain 1997;120:141-57.

11. Dukart J, Mueller K, Horstmann A, Vogt B, Frisch S, Barthel H, et al. Differential effects of global and cerebellar normalization on detection and differentiation of dementia in FDG-PET studies. Neuroimage 2010; 49:1490-5.

12. Kushner M, Tobin M, Alavi A, Chawluk J, Rosen M, Fazekas F, et al. Cerebellar glucose consumption in normal and pathologic states using fluorine-FDG and PET. J Nucl Med 1987;28:1667-70.

13. Watanabe T, Honda Y, Fujii Y, Koyama M, Matsuzawa H, Tanaka R. Three-dimensional anisotropy contrast magnetic resonance axonography to predict the prognosis for motor function in patients suffering from stroke. J Neurosurg 2001;94:955-60.